First publ. in: Journal of Histochemistry and Cytochemistry 52 (2004), 12, pp. 1543-1559

Immunolocalization of Actin in *Paramecium* Cells

Roland Kissmehl, Ivonne M. Sehring, Erika Wagner, and Helmut Plattner

Department of Biology, University of Konstanz, Konstanz, Germany

SUMMARY We have selected a conserved immunogenic region from several actin genes of *Paramecium*, recently cloned in our laboratory, to prepare antibodies for Western blots and immunolocalization. According to cell fractionation analysis, most actin is structure-bound. Immunofluorescence shows signal enriched in the cell cortex, notably around ciliary basal bodies (identified by anti-centrin antibodies), as well as around the oral cavity, at the cytoproct and in association with vacuoles (phagosomes) up to several μm in size. Subtle strands run throughout the cell body. Postembedding immunogold labeling/EM analysis shows that actin in the cell cortex emanates, together with the infraciliary lattice, from basal bodies to around trichocyst tips. Label was also enriched around vacuoles and vesicles of different size including "discoidal" vesicles that serve the formation of new phagosomes. By all methods used, we show actin in cilia. Although none of the structurally well-defined filament systems in *Paramecium* are exclusively formed by actin, actin does display some ordered, though not very conspicuous, arrays throughout the cell. F-actin may somehow serve vesicle trafficking and as a cytoplasmic scaffold. This is particularly supported by the postembedding/EM labeling analysis we used, which would hardly allow for any large-scale redistribution during preparation. **(J Histochem Cytochem 52:1543–1559, 2004)**

KEY WORDS
actin
cilia
immunolocalization
microfilaments
vesicle traffic
Paramecium

ACTIN IS A HIGHLY FLEXIBLE cytoskeletal component that participates in many static and dynamic functions in eukaryotic cells (Pollard et al. 2000). This includes reversible self-assembly of monomeric G-actin to F-actin filaments. Also generally known is that these filaments may be more or less bundled and can serve different functions, such as structural enforcement and restructuring of the cell cortex, rearrangement of cortical components during intracellular signaling, organelle dynamics and transport, etc. The latter includes well-established functions such as phagosome formation and plasma streaming, i.e., cyclosis (Shimmen and Yokota 2004). However, quite recent results highlight a much broader functional spectrum of F-actin than previously assumed. This applies to early steps of exocytosis, including dense core vesicle docking (Morales et al. 2000; Pendleton and Koffer 2001; Manneville et al. 2003; Gasman et al. 2004), late steps of endocytosis (Engqvist-Goldstein and Drubin 2003; Guilherme et al. 2004), exo-endocytosis coupling (Valentijn et al. 1999), endo-phagosome interaction (Kjeken et al. 2004), delivery of endocytosed receptors to lysosomes for degradation (Stoorvogel et al. 2004), vacuole fusion in yeast (Merz and Wickner 2004), and positioning of the nucleus (Starr and Han 2003). Some aspects are still poorly understood, particularly, e.g., the role of actin in flagella of algae (Mitchell 2000; Hayashi et al. 2001; Hirono et al. 2003), whereas its occurrence in cilia has remained a matter of debate. Another line of experiments concerns the potential role of actin in mediating the connection between cortical Ca^{2+}-stores and the plasma membrane (Patterson et al. 1999; Rosado and Sage 2000; Kunzelmann-Marche et al. 2001; Wang et al. 2002).

Different actin isoforms occurring in many organisms may serve specific functions in the respective cells (Pollard et al. 2000; Wagner et al. 2002). For localization, antibodies (ABs) may be used at the light microscope (LM) and electron microscope (EM) levels, as well as for Western blots. Bicyclic peptide toxins, phalloidin or jasplakinolide, can bind rather specifically to F-actin, thus allowing fluorescence labeling (Wieland and Faulstich 1978; Bubb et al. 2000). This or the alternative approach, F-actin disruption by toxins of the

Correspondence to: H. Plattner, Department of Biology, University of Konstanz, P.O. Box 5560, 78457 Konstanz, Germany. E-mail: helmut.plattner@uni-konstanz.de

Received for publication May 10, 2004; accepted August 13, 2004 [DOI: 10.1369/jhc.4A6379.2004].

type cytochalasin B and D or latrunculin A, is also widely used for functional analyses also with ciliates (see below).

In previous times, mainly before molecular biology approaches could be undertaken, biochemical, functional, and immunolocalization studies were tried to probe the potential function of F-actin in ciliates such as *Paramecium* (Tiggemann and Plattner 1981; Cohen et al. 1984; Fok et al. 1985; Kersken et al. 1986a,b), *Tetrahymena* (Mitchell and Zimmerman 1985; Hirono et al. 1987b,1989; Hoey and Gavin 1992), *Pseudomicrothorax* (Hauser et al. 1980), *Histriculus* (Pérez-Romero et al. 1999), *Climacostomum* (Fahrni 1992), and *Spirostomum* (Zackroff and Hufnagel 1998). However, with ciliates, F-actin–disrupting drugs frequently had to be used in conspicuously high concentrations to abolish, e.g., phagocytosis (Fok et al. 1987; Zackroff and Hufnagel 1998,2002). With a variety of protozoa of the phylum Alveolata, actin genes or partial sequences of it have been cloned. This holds in particular for ciliates, such as *Tetrahymena* (Zimmerman et al. 1983; Cupples and Pearlman 1986; Hirono et al. 1987a) and *Paramecium* (Díaz-Ramos et al. 1998), but also for their pathogenic relatives of the group of Apicomplexa such as *Toxoplasma* (Delbac et al. 2001).

Our present analysis also addresses some special subcellular structures in *Paramecium* cells that contain multiple filament systems (Allen 1971; Cohen et al. 1984,1987; Cohen and Beisson 1988; Keryer et al. 1990a,b; Allen et al. 1998; Beisson et al. 2001; Clérot et al. 2001). We focus on regions with dense-core secretory vesicles ("trichocysts"), cortical filament bundles ("infraciliary lattice," cf. Allen 1971,1988), the narrow space between the plasma membrane and tightly attached cortical Ca^{2+}-stores ("alveolar sacs," see Plattner and Klauke 2001), in addition to abundant vesicles of the phago-/lysosomal and recycling system (Fok and Allen 1990; Allen and Fok 2000). Recent cloning of several actin genes of *Paramecium tetraurelia* in our laboratory opened up a new way to structural localization with this cell, whose regular "design" facilitates such studies. So far, studies on actin in *Paramecium* have not addressed all relevant aspects, and many aspects have remained controversial.

Materials and Methods

Stocks and Cultures

The wild-type strain of *P. tetraurelia* used was stock 7*S*. Cells were cultivated in a decoction of dried lettuce monoxenically inoculated with *Enterobacter aerogenes* as a food organism, supplemented with 0.4 $\mu g \cdot ml^{-1}$ β-sitosterol (Sonneborn 1970). For subcellular fractionation, we used axenic cultures (Kaneshiro et al. 1979). Cells were grown at 25C to early stationary phase as previously described (Kissmehl et al. 1996).

Expression of *Paramecium* Actin-specific Peptides in *Escherichia coli*

For heterologous expression of actin-specific peptides we selected the amino acid sequence of actin1-1 (accession number AJ537442). After changing all deviant *Paramecium* glutamine codons (TAA and TAG) into universal glutamine codons (CAA and CAG) by PCR methods, the coding regions of either E57-P243 (N-terminal region) or L251-G366 (C-terminal region) of *Paramecium* actin1-1 were cloned into the XhoI/BamH1 restriction sites of pET 16b expression vector of the pET System from Novagen (Madison, WI) which employs a His_{10} tag for purification of the recombinant peptides.

Purification of Recombinant Actin1-1 Peptides

Recombinant actin1-1 peptides, actin1-$1_{E57\text{-}P243}$ and actin1-$1_{L251\text{-}G366}$ were purified by affinity chromatography on Ni^{2+}-nitrilotriacetate agarose under native conditions, as recommended by the manufacturer (Novagen). The recombinant peptides were eluted with a step gradient, 100 to 1000 mM imidazole in 50 mM sodium phosphate (pH 6.0) with 300 mM NaCl added. The fractions collected were analyzed on SDS polyacrylamide gels, and those containing the recombinant peptides were pooled and dialyzed in phosphate-buffered saline (PBS).

Antibodies Used

ABs against the two recombinant actin peptides, actin1-$1_{E57\text{-}P243}$ and actin1-$1_{L251\text{-}G366}$, were raised either in rabbits or mice. After several boosts, positive sera were taken at day 60 and purified by two subsequent chromatography steps, a first step on a His-tag peptide column (24-amino acid peptide, to remove His tag-specific ABs), followed by an affinity step on the corresponding actin1-1 peptide. One of these ABs recognizes the N-terminal and the other the C-terminal region of actin1-1, yet results achieved in this study were indistinguishable with either type of ABs. Therefore, no further distinction is made, unless indicated. We used the sequence of *Paramecium* actin 1-1 because it is rather similar for numerous isoforms that we have cloned (R. Kissmehl, J. Mansfeld, E. Wagner, I. Sehring, H. Plattner, unpublished data) and thus should allow us to establish an overall distribution of actin, notably of F-actin, in *Paramecium*.

Mouse polyclonal ABs against *Paramecium* actin1-1 were selectively used for the colocalization at the LM level, in conjunction with an anti-centrin (*Dictyostelium discoideum*) polyclonal AB produced in rabbits (designation HisDd-Centrin2 from R. Gräf, University of Munich) used to identify ciliary basal bodies (Daunderer et al. 2001).

Cell Fractionation

Cells were deciliated by a Mn^{2+}-shock (for details, see below) and cilia were purified by differential centrifugation (Nelson 1995). Whole-cell homogenates were prepared in phase buffer (20 mM Tris-maleate, 20 mM NaOH, 20 mM NaCl, 250 mM sucrose, pH 7.0) by ~100 hand strokes in a glass homogenizer equipped with a Teflon pestle. Soluble and particulate fractions were separated by centrifugation at 100,000 × g for 60 min at 4C. Cell surface complexes ("cortices") were prepared according to Lumpert et al. (1990),

and trichocysts were isolated by the method of Glas-Albrecht and Plattner (1990). A protease-inhibitor cocktail containing 15 μM pepstatin A, 100 mU/ml aprotinin, 100 μM leupeptin, 0.26 mM TAME, 28 μM E64, and 0.2 mM Pefabloc SC was used throughout.

Electrophoretic Techniques and Western Blot Analysis

Protein samples were denatured by boiling for 3 min in sample buffer (0.4 M Tris–HCl, 1% SDS, 0.5% DTT, 20% glycerol, pH 8.0) and subjected to electrophoresis on linear gradient (5–20%) SDS polyacrylamide gels using the discontinuous buffer system of Laemmli (1970). Before electrophoresis, samples were alkylated for 30 min at 20C by 2% iodoacetamide. Protein standards were used in accordance with manufacturer directions. Gels were either stained with Coomassie blue R250 or prepared for electrophoretic protein transfer onto nitrocellulose membranes. Protein blotting was performed at 2 mA/cm^2 for 1 hr according to the technique of Kyhse-Andersen (1989) using the semidry blotter from BioRad (Munich, Germany). ABs were diluted 1:1000 in 0.25% (w/v) non-fat dry milk and Tris-buffered saline, pH 7.5, and applied overnight at 4C. AB binding was visualized by a second AB coupled to alkaline phosphatase (Sigma: Taufkirchen, Germany) using 5-bromo-4-chloro-3-indolyl phosphate and Nitro Blue tetrazolium as substrates.

Immunofluorescence Labeling

Basic Procedure. Cells were washed twice in 5 mM Pipes buffer, pH 7.0, containing 1 mM KCl and 1 mM $CaCl_2$. Cells were fixed in 4% (w/v) freshly depolymerized formaldehyde for 20 min at room temperature. Cells were then permeabilized and fixed in a mixture of 0.5% digitonin and 4% formaldehyde, dissolved in 5 mM Pipes buffer, pH 7.0, for 30 min. Cells were washed twice in PBS, 2 × 10 min in PBS with 50 mM glycine added and 30 min in this solution with 1% bovine serum albumin (BSA) added. The rabbit anti-actin AB was applied in a dilution of 1:50 in PBS (+1% BSA) for 90 min at room temperature. After 4 × 15 min washes in the same solvent, FITC-conjugated anti-rabbit ABs, diluted 1:50, were applied for 90 min, followed by 4 × 15 min washes in PBS. Samples were shaken gently during all incubation and washing steps.

Deciliated Cells. Cells were washed twice in 5 mM Pipes buffer, pH 7.0, each containing 1 mM KCl and $CaCl_2$, at room temperature and suspended in 50 mM $MnCl_2$ solution in 10 mM Tris-HCl, pH 7.2. After 2 min at 4C, cells were removed by centrifugation and resuspended in the same solution. After 10 min of gentle shaking, 90–95% of cells were deciliated. Deciliated cells were removed by centrifugation and washed twice in Pipes buffer before further use.

Deciliated cells were fixed in 8% (w/v) freshly depolymerized formaldehyde with 0.5% digitonin, 1 mM ATP, 10 mM $MgCl_2$, and 10 mM KCl added, for 20 min on ice in Pipes buffer, pH 7.0. After fixation, cells were washed twice in PBS, 2 × 10 min in PBS with 50 mM glycine added and 30 min in this solution with 1% BSA added. The mouse anti-actin AB was applied in a dilution of 1:50 in PBS (+1% BSA) for 90 min at room temperature. After 4 × 15 min washes in the same solvent, FITC-conjugated anti-mouse ABs, diluted 1:50, were applied for 90 min, followed by 4 × 15 min washes in PBS. A second labeling with anti-centrin ABs from rabbits was performed as described above, using Texas Red–conjugated anti-rabbit ABs. Anti-rabbit and anti-mouse fluorescent AB conjugates were from Sigma-Aldrich (St Louis, MO) and Serva (Heidelberg), respectively.

Light Microscopy. Cells were mounted with Mowiol supplemented with n-propylgallate to reduce fading. To analyze fluorescence staining, we used a conventional LM, type Axiovert 100TV (Zeiss; Oberkochen, Germany), or a confocal laser scanning microsope (CLSM) type LSM 510 (Zeiss) equipped with a Plan-Apochromat ×63 oil immersion objective (numeric aperture 1.4). Images acquired with the LSM 510 software were processed with Photoshop software (Adobe Systems, San Jose, CA).

Fixation and Embedding for Postembedding EM Analysis

Using a quenched-flow apparatus (Knoll et al. 1991), *Paramecium* cells were rapidly injected into 8% formaldehyde plus 0.1% glutaraldehyde dissolved in Pipes buffer, pH 7.2 (0C), with 1 mM KCl and $CaCl_2$ each added, further fixed for 60 min at 4C, washed in PBS (pH 7.4) + 50 mM glycine (2 × 10 min), dehydrated by increasing ethanol concentrations (30%, 50%, 70%, 90%, 96%, 2 × 15 min each, and 2 × 100%, 30 min each), and impregnated with LR Gold resin (London Resin, London, UK) at 0C, with two changes in 2-hr intervals each and then overnight, followed by UV-light polymerization at −35C for 72 hr.

Immunogold Labeling and EM Analysis

Postembedding Method. Ultrathin sections mounted on formvar-coated Ni grids were pretreated (2 × 10 min) with 20 μl of PBS, then for 10 min with PBS with 50 mM glycine added, and finally immersed in PBS supplemented with 0.5% BSA and 0.5% goat serum (2 × 10 min, room temperature), to eliminate nonspecific gold adsorption. Grids were then incubated with rabbit AB, diluted 1:20 in PBS supplemented with 0.3% BSA-c (BioTrend, Köln, Germany), pH 7.4, 1 hr at room temperature. BSA-c as an acetylated form reduces nonspecific adsorption of gold conjugates due to increased net charge.

Samples were washed in PBS/BSA-c (0.3%) three times, 10 min each, and treated for 1 hr with gold conjugates. We used goat anti-rabbit IgGs coupled to gold of 5 nm (Au_5) provided by Sigma, diluted 1:30.

Preembedding Labeling. Without exception, cells were fixed with 8% formaldehyde + 0.1% glutaraldehyde and simultaneously treated with digitonin (Sigma) and the other additives, as described above for LM analysis of deciliated cells, incubated with primary rabbit ABs against *Paramecium* actin1-1, followed by Au_5-conjugated second ABs, with the aim to make the narrow subplasmalemmal space accessible. After embedding in LR Gold (London Resin), sections were additionally subjected to the postembedding labeling procedure with the same primary and secondary ABs, respectively.

Specificity of Immunogold Labeling and Further Processing. This was verified by the significant reduction of the number of Au_5 particles on sections incubated with ABs that had been preadsorbed with the original antigen.

Further Processing and Quantitative Evaluation. After labeling, sections were rinsed with distilled water, fixed for 5 min with 2% glutaraldehyde, and routinely stained for 3 min with 2% aqueous uranyl acetate (unbuffered, pH ~4.5). EM micrographs were taken at defined magnifications and enlarged to ×77,000. Au_5 grains were counted and referred to area size determined by superposition of square lattices with 5, 10.0 and 20.0 mm spacing, respectively, depending on the size of the structure to be analyzed (Plattner and Zingsheim 1983). The actual area sizes to which the numbers of gold grains were referred were determined from the number of hit points.

Results

Actin-specific ABs, Cell Fractionation, and Western Blot Analysis

Molecular cloning from a pilot sequencing project (Dessen et al. 2001; Sperling et al. 2002) as well as from the ongoing *Paramecium* genome project of the Groupement de Recherche Européen at the Genoscope (Evry, France) revealed that *P. tetraurelia* contains an actin multigene family with at least 30 members, all encoding actin and actin-related proteins with calculated molecular masses ranging between 38 and 45 kD (R. Kissmehl, J. Mansfeld, I. Sehring, E. Wagner, H. Plattner, unpublished data). One of them, actin 1-1 (accession number AJ537442), a member of the actin-1 subfamily with rather conserved immunogenic regions (Figure 1), was chosen for heterologous expression in *E. coli* (after changing all deviant *Paramecium* glutamine codons into universal glutamine codons) and subsequent production of polyclonal ABs. Various polyclonal ABs were raised against the N-terminal (E57-P243) or C-terminal region (L251-G366, Figure 1), all readily recognizing the recombinant peptides used for immunization when tested in slot blots and Western blots (data not shown). After affinity purification, the actin-specific ABs were further characterized in ELISA and Western blots. Results obtained were similar, whether ABs were used against the N-terminal or the carboxy-terminal region of actin 1-1, confirming their high specificity against actin or actin-specific peptides (data not shown). The following analyses, including Western blots, and LM and EM analyses, have been performed predominantly with ABs against the C-terminal region of *Paramecium* actin1-1 (Figure 1).

Western blots from homogenates display a strong band of 43 kD and a weak one of 40 kD (Figure 2). Such bands also occur in the 100,000 × g pellet, while the 43 kD band is much weaker in the 100,000 × g supernatant. The 43 kD band is typical of actin, while the 40 kD band may represent one of the shorter isoforms of the actin or actin-related gene products of *Paramecium* (Kissmehl et al., unpublished data). A 43-kD band also clearly occurs in cilia and in cortices, while it is hardly discernible in the trichocyst fraction. Both the 100,000 × g supernatant and pellet also display some very weak bands of lower size, possibly

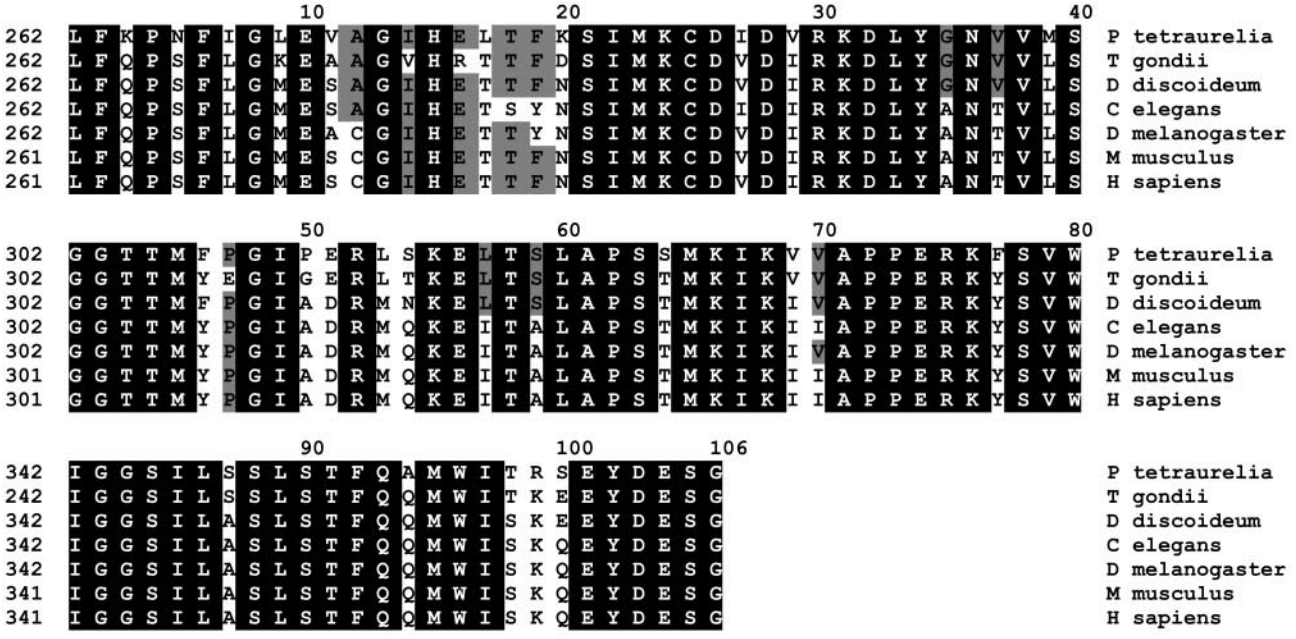

Figure 1 Multiple alignment of the C-terminal region of *Paramecium* actin1-1. Actin-specific sequences from *Paramecium tetraurelia* (AJ537442), *Toxoplasma gondii* (P53476), *Dictyostelium discoideum* (AA052255), *Caenorhabditis elegans* (X16797), *Drosophila melanogaster* (NP_523625), *Mus musculus* (NP_033739), and *Homo sapiens* (AAH16045) were aligned using the CLUSTALW program. Identical residues are shaded (black), while lesser conserved positions are labeled greyish.

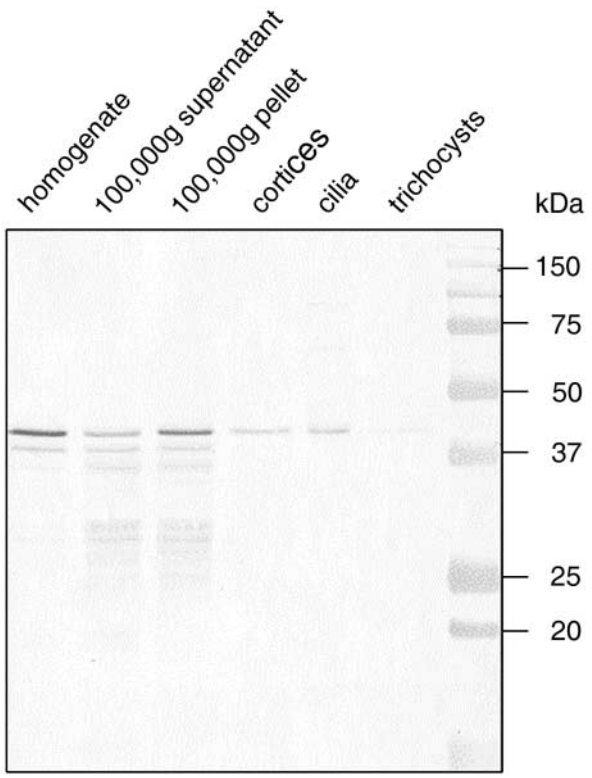

Figure 2 Western blot using affinity-purified anti-actin (*Paramecium* type 1-1) ABs showing a prominent band of 43 kD in the homogenate and in the fractions indicated, except trichocysts. This band represents preferably structure-bound actin (100,000 × g pellet) and appears also in isolated cortex and ciliary fractions. Note a fainter band of 40 kD in the homogenate and in the 100,000 × g supernatant and pellet, which both contain further weak bands of lower mass (possibly degradation products or cross-reacting actin-related proteins). Right lane: molecular mass markers.

generated by partial proteolysis during fractionation. None of the bands were visible when Western blots were produced with the corresponding preimmune sera or in controls with the second AB alone (data not shown).

Immunofluorescence Labeling

To account for some variability in the immunofluorescence staining, we present typical extremes of CLSM images from double labeling experiments (Figures 3A–3D), with mouse anti-actin FITC-ABs and rabbit anti-centrin Texas Red-ABs, the latter specific for the centrosome in *Dictyostelium* (Daunderer et al. 2001) and basal bodies in *Paramecium*. This is in contrast to the pattern obtained by the monoclonal AB 20H5 against centrin from *Chlamydomonas* (Sanders and Salisbury 1994) which in *Paramecium* brilliantly stains not only basal bodies but also the infraciliary lattice (Klotz et al. 1997; Beisson et al. 2001). Labeling with both anti-actin and anti-centrin ABs in part coincides with ciliary basal bodies of the outer cell surface and along the oral cavity, the outline of the oral cavity, and on the cytoproct. This structure is identified by its "poster-ovental" position, size, and shape (Allen 1988). The degree of coincidence (yellow) on basal bodies and in the oral cavity may vary; e.g., it is higher in Figures 3A and 3B than in Figures 3C and 3D. The gradient of coincidence in Figure 3A indicates some differential positioning of the respective antigens along the z-axis.

Figure 3B shows the occurrence of actin around vesicles and vacuoles of various sizes, whereas the position of the red-labeled structures may suggest coincidence with elements of the osmoregulatory system—aspects that have not been followed in any more detail. Figure 3D documents more clearly a cortical actin layer and actin filaments throughout the cytoplasm, frequently in a radial arrangement, and sometimes with local concentration.

We used conventional LM analysis to analyze immuno-FITC labeling of cilia with anti-actin ABs (Figure 4), thus taking advantage of a thicker optical section layer. While intracellular details are largely blurred, ciliary basal bodies and cilia on the outer cell surface are clearly labeled. This may also apply to cilia in the oral cavity, although this is not resolved in Figure 4.

Comparative Analysis of CLSM and Immunogold EM Labeling

For most results achieved by CLSM analysis, we find equivalents in the immunogold EM analyses (Figures 5 to 11), as specified below and summarized in Table 1. Off-cell background is low [2.15 gold grains per $\mu m^2 \pm 0.85$ (SEM)], as it is on irrelevant structures, such as mitochondria, trichocyst contents, and alveolar sacs (2.2, 1.4, and 0.3 gold grains per μm^2, respectively).

After postembedding labeling, gold granules are scattered, yet with specific concentration zones over the cytosolic compartment. This holds for the cell cortex (Figures 6 to 8) with its ciliary basal bodies, as well as for regions adjacent to the oral cavity, including a zone enriched in ciliary basal bodies (Figure 10A) and a zone enriched in recycling vesicles (discoidal vesicles) dedicated to phagosome formation (Figure 10B). It also holds for regions deeper inside the cytoplasm where elements of vesicle trafficking are enriched (Figure 11). Cilia are also labeled at the EM level (Figures 5 and 10, Table 1), just as with the other methods used (Figures 2 and 4). In sum, there is good agreement between LM and EM labeling. Because the cytoproct shows up rarely, we were unable to analyze it at the EM level.

Figure 9 represents experiments with digitonin-permeabilized cells, showing AB-gold labeling in the narrow subplasmalemmal space between the plasmalemma

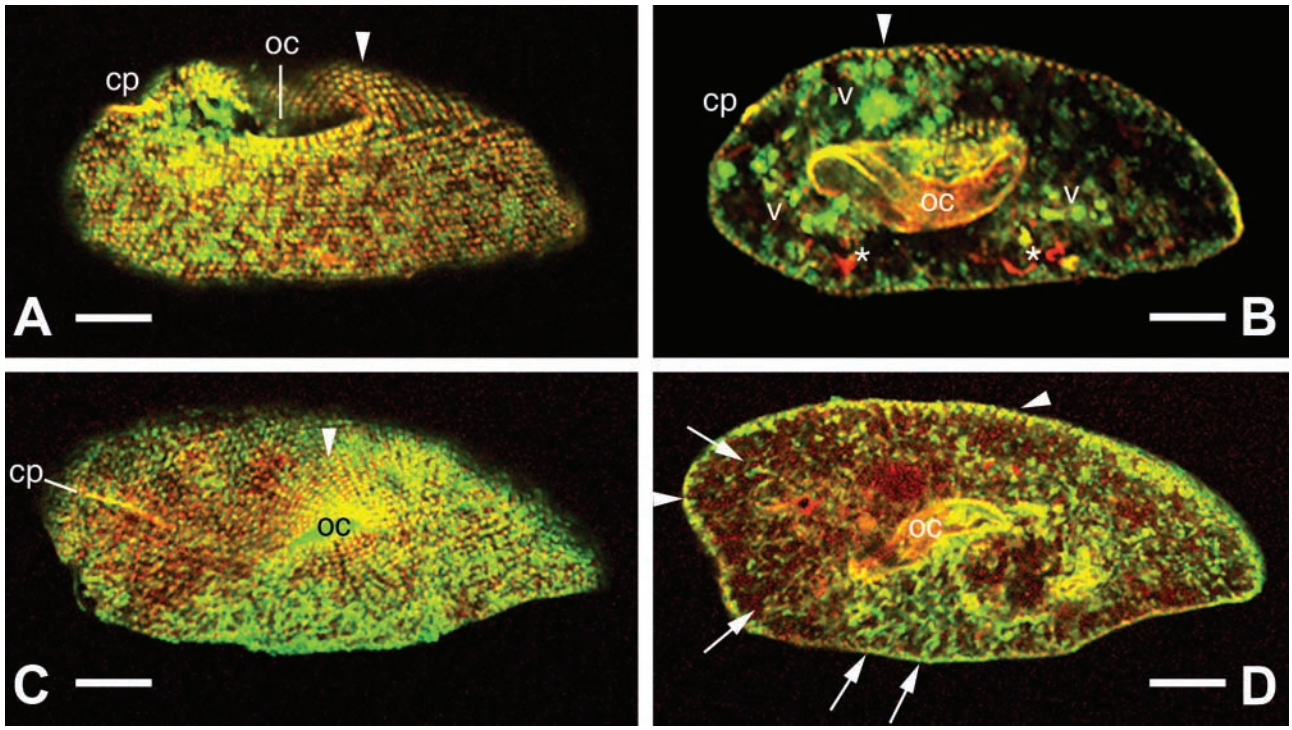

Figure 3 Colocalization of actin and centrin (yellow) by CLSM using mouse ABs against actin (green) and rabbit ABs against centrin (red). Two deciliated cells (**A,B** vs **C,D**) showing extreme situations of labeling are presented. (**A,C**) are superficial sections; (**B,D**) are median focal planes. Note colocalization at basal bodies in top-most focal planes (arrowheads), on the cytoproct (cp) and in parts of the oral cavity (oc). Basal bodies located in layers outside the optical section are preferably red (**A**) or green (**C**), thus suggesting a layered arrangement of actin and centrin in these regions of the cell. Note occurrence of actin in the outermost cortex layer particularly in (**D**, arrowheads) as well as of interior actin clusters probably associated with vacuoles (v in **B**) and as filament bundles indicated by arrows (**D**). (**B**) displays centrin staining at two conspicuous sites where the osmoregulatory system is located (asterisks) and actin labeling associated with large vacuoles (v). Bars = 10 μm.

and the outer side of alveolar sacs, while there is only spurious label occasionally seen after mere section labeling (Figures 5 and 7). Apart from this aspect, little label only is seen in the cell cortex with permeabilized cells (Figure 9). While digitonin permeabilization may be more appropriate than section labeling to show the presence of some actin in the very narrow outermost cytosolic space, particularly when enhanced by additional postembedding labeling (Figure 9), it may cause a serious overall loss of antigen. The abundance of

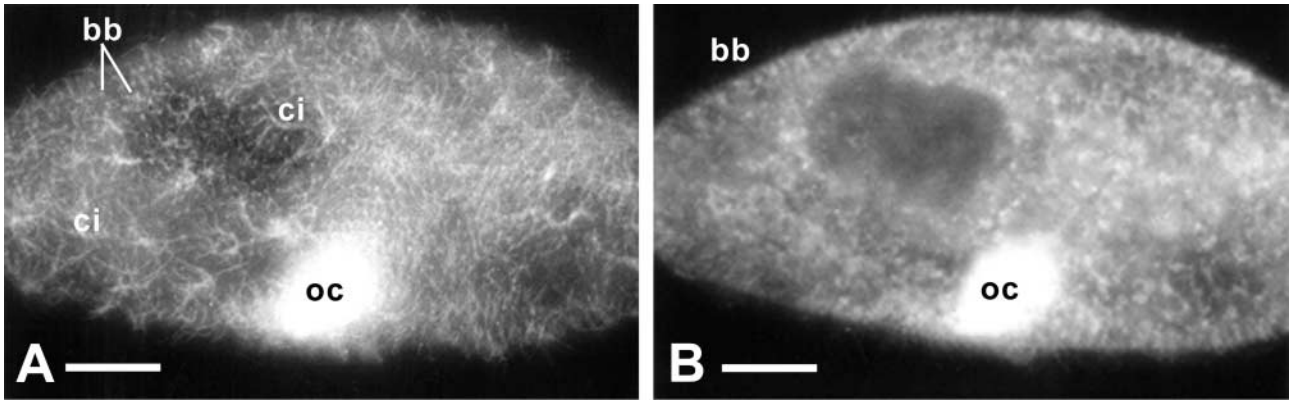

Figure 4 Conventional anti-actin AB-fluorescence image of a cell permeabilized under conditions preserving cilia. (**A**) superficial, and (**B**) median plane. Note labeling of cilia (ci) in (**A**) and of their basal bodies (bb) in (**A,B**), of specks and strands in (**B**), and of the presumable oral cavity (oc) in (**A,B**). Bars = 10 μm.

cortical label after postembedding labeling justifies reliance in this study mainly on the postembedding procedure for further evaluation. Concomitantly, all figures presented with the exception of Figure 9 were obtained by this method.

Specification of Results Obtained with Postembedding Labeling

Beyond the general labeling of the cytosolic compartment of the cell cortex (Figures 5 to 8), we recognize that gold granules are enriched to a variable extent in a variety of structures.

The cytoplasm of cell surface ridges, typical of ciliated protozoa, are labeled (Figures 5 and 6). This also holds for the cytoplasm surrounding the tips of the elongate trichocyst organelles, as shown in cross-section (Figures 5 and 6) and in longitudinal section (Figure 7). The gold label associated with cortical basal bodies is somewhat variable and may in part sit inside this structure, as shown particularly in Figure 8B, where it shows up below the basal plate (Figure 8A). Gold label also occurs adjacent to cortical basal bodies, e.g., in the filamentous mass in Figure 6. This material is associated with the origin of a kinodesmal fiber emanating from a basal body from where the infraciliary lattice also emanates. From there, these filament bundles pass near adjacent trichocyst tips (Figure 5), as established by Allen (1971,1988). Although the bulk of the latter filament system is made of centrin (Beisson et al. 2001), some actin clearly appears to be associated with it. Gold label also surrounds ghosts from discharged trichocysts (Figure 6).

Table 1 summarizes labeling densities on a quantitative level (gold grains per μm^2). These are, in decreasing magnitude, as follows: 301.0 Au/μm^2 for cytoplasmic regions around oral cavity and around food vacuoles, 141.5 for cell surface ridges, 111.9 for immediate surroundings of trichocysts, between 89.5 and 95.6 for infraciliary lattice, ciliary basal bodies, and cilia, followed by cortical cytoplasm (37.8) and the complex formed by the plasma membrane and the outer alveolar sacs membrane (25.9 Au/μm^2). For statistics, see Table 1.

While the abundant filament bundles located in the cytoplasm around the oral cavity are made of materials other than actin (see "Discussion"), the distinct labeling in between such bundles (Figure 10A) again indicates association with actin. As in the cell cortex, some label may be associated with ciliary basal bodies around the oral cavity. Furthermore, we find intense labeling of cytosolic regions enriched in vesicles accumulated near the cytopharynx (Figure 10B). Many are oblong and thus represent discoidal vesicles known to serve membrane recycling from the cytoproct, i.e., formation of new phagocytic vacuoles (Fok and Allen 1988; Allen and Fok 2000). In these domains of the cell, less labeling is seen immediately below the cell membrane than between the adjacent round and discoidal vesicles.

Deeper inside the cell, small vesicles of different diameters are embedded in considerably labeled cytosol, frequently in close association with a large vacuole (Figures 11A and 11B). This arrangement suggests their identity either as lysosomes or as acidosomes in typical arrangement with phagosomes. These interpretations are suggested by the work of Allen and Fok (2000); e.g., considering the flat shape of the large vacuole indicating an early biogenetic stage of a food vacuole. Figure 11B shows association of actin label with parallel microtubular aggregates, the gold label unilaterally concentrated at sites where microtubules enter the section plane. Also in Figure 11B, a heavily labeled "trail" is in direct extension of the adjacent microtubular bundle. This indicates involvement of actin in phago-lysosomal vesicle trafficking, although after the preparation protocol required for immunogold analysis, distinct filaments are difficult to recognize. However, some of these gold aggregates may be the equivalent of the fluorescent strands visualized by anti-actin ABs in Figure 3.

Discussion

Background from Previous Work

Occurrence of most actin in *Paramecium* in structure-bound form contrasts with the abundance of monomeric actin in Apicomplexa (Sibley 2004), including *Toxoplasma* (Poupel et al. 2000; Wetzel et al. 2003). This makes fluorescence labeling studies with F-actin–specific drugs feasible. In *Paramecium*, phalloidin, heavy meromyosin, and DNaseI have clearly revealed labeling of the cell cortex, particularly of ciliary basal bodies (Tiggemann and Plattner 1981; Kersken et al. 1986a,b). Phalloidin also has labeled the nascent food vacuole (Kersken et al. 1986a,b). Concomitantly, cytochalasin B has been reported to inhibit formation of phagocytic vacuoles (Allen and Fok 1983,1985; Fok and Allen 1988). It also inhibits docking of trichocysts (Beisson and Rossignol 1975), and it even can detach docked trichocysts from the cell surface (Pape and Plattner 1990). When phagocytosis has been analyzed with different F-actin–disrupting drugs and analogs, respectively, the requirement of concentrations well above those used with mammalian cells has been confirmed (Beisson and Rossignol 1975; Pape and Plattner 1990; Zackroff and Hufnagel 1998). This is in line with the low sensitivity of F-actin in other ciliates. In total, these data are all compatible with our current results obtained with ABs against the original *Paramecium* antigen.

Previous attempts to localize actin in *Paramecium* have led to controversies. One discrepancy concerned

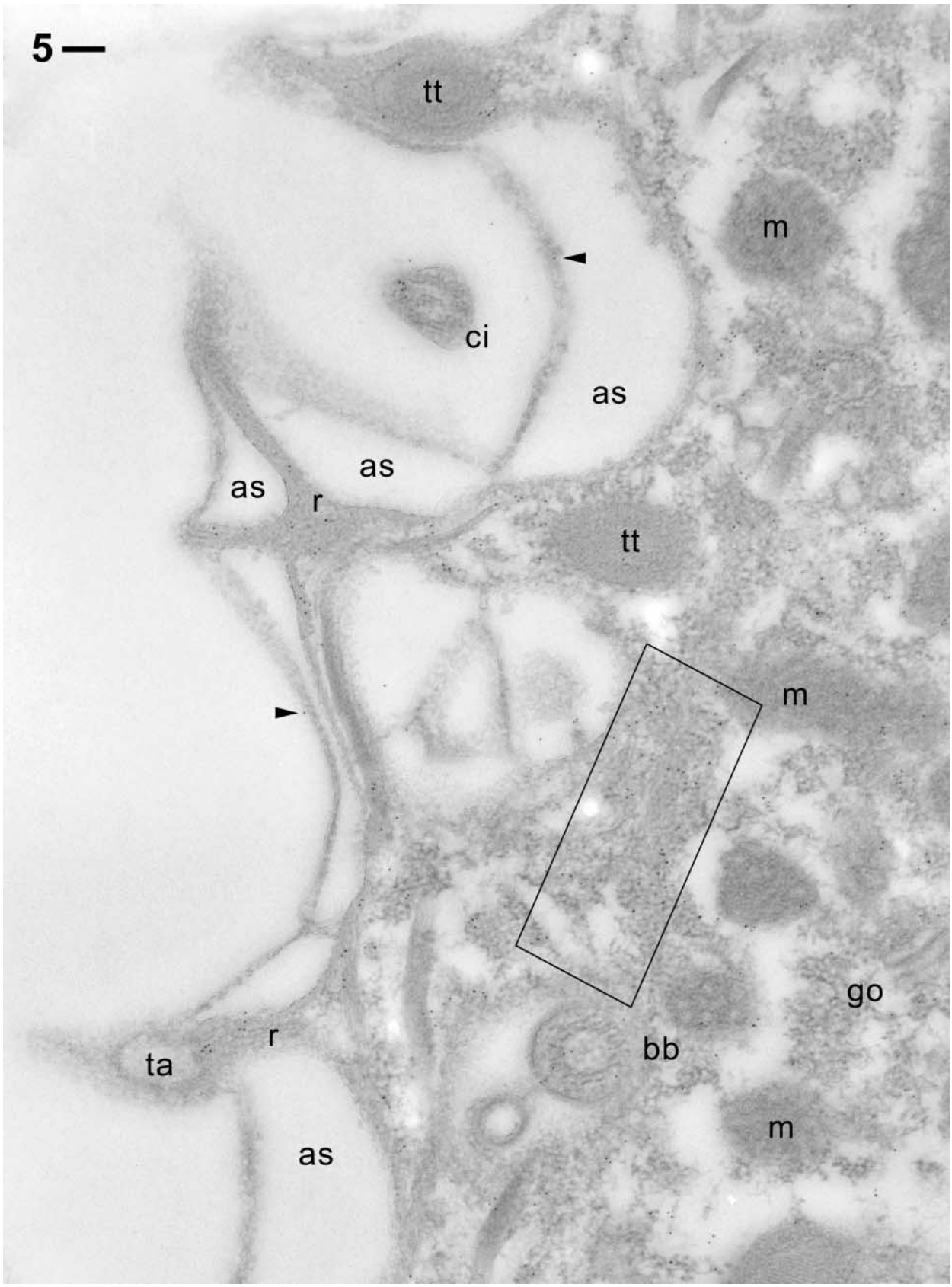
5
tt
m
ci
as
as
as
r
tt
m
go
r
bb
ta
m
as

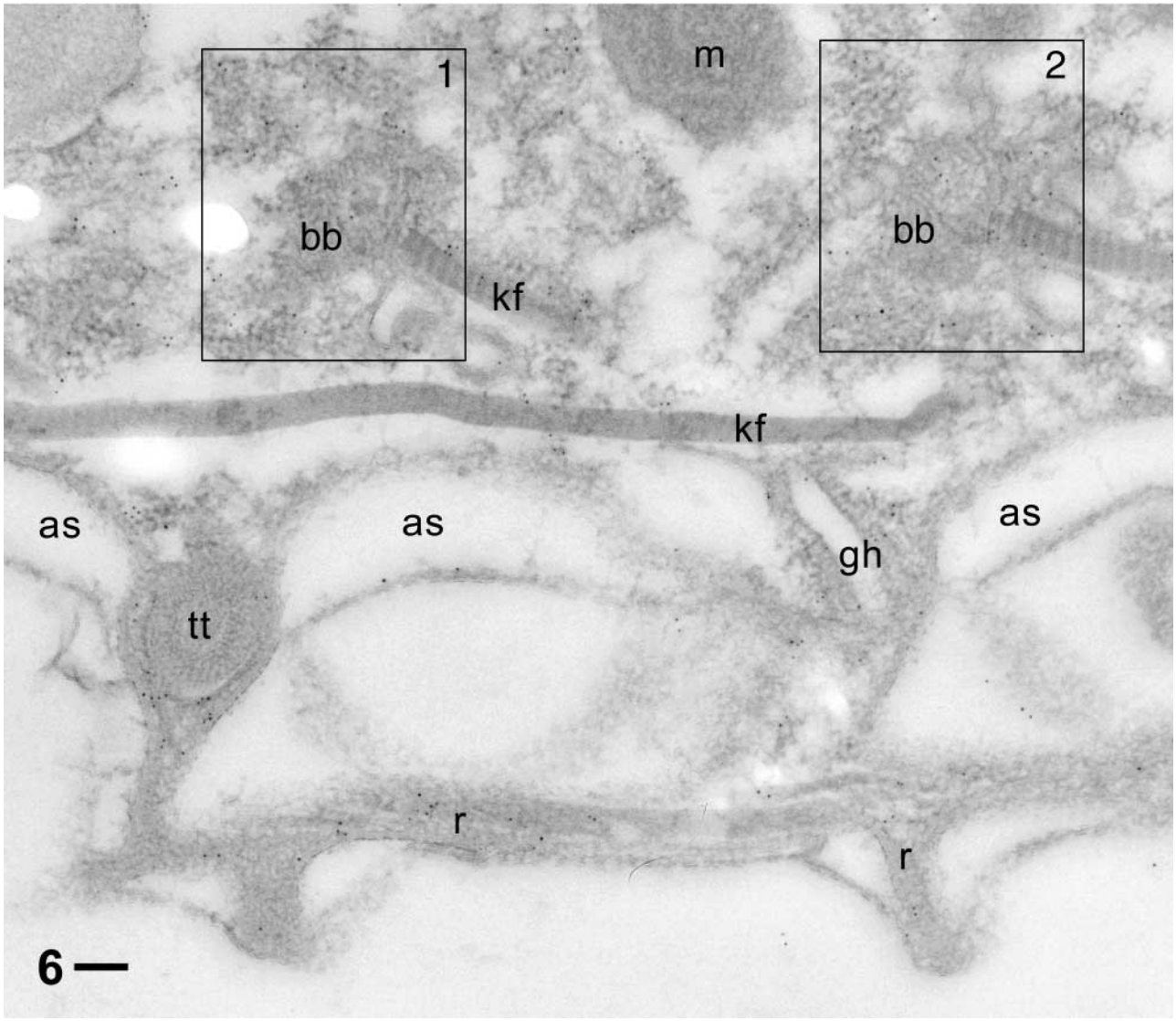

Figure 6 Similar situation as in Figure 5, but in addition with more distinct label around a trichocyst tip (tt) and a ghost (gh) from a released trichocyst, and much less in diffuse association (frames 1, 2) with two basal bodies (bb) from which typically kinodesmal fibers (kf) originate. Cell surface ridges (r) are also labeled. Note almost absence of label outside the cell or inside alveolar sacs (as), the trichocyst tip and ghost, as well as in a mitochondrion (m). Bar = 0.1 μm.

the composition of cortical filament bundles, notably of the infraciliary lattice emanating from ciliary basal bodies. While the bulk of this filament system has been established as centrin (Beisson et al. 2001), this does not necessarily preclude association of centrin filaments with actin, as we can show. Recall that widely different affinity stains for actin, including heavy meromyosin, have resulted in cortical labeling in *Paramecium* (Tiggemann and Plattner 1981; Kersken et al. 1986a,b), as well as in *Tetrahymena* (Méténier 1984). Theoretically, previous LM and preembedding-EM localization studies could have faced the problem of sol-

Figure 5 Postembedding immunogold labeling in the cell cortex. Note almost absence of background outside the cell and within membrane-bound organelles such as alveolar sacs (as), trichocyst tips (tt), mitochondria (m), and a Golgi field (go). This is in contrast to the occurrence of clear, though scattered, labeling of cytoplasmic ridges (r) typical of the *Paramecium* cell surface, around a trichocyst tip (top) and close to a trichocyst attachment site (ta), in a cilium (ci), in a ciliary basal body (bb), and along filamentous materials emanating from there (rectangle), probably infraciliary lattice. Note a single gold grains (arrowheads) on the complex formed by the cell membrane and the outer side of an alveolar sac. Bar = 0.1 μm.

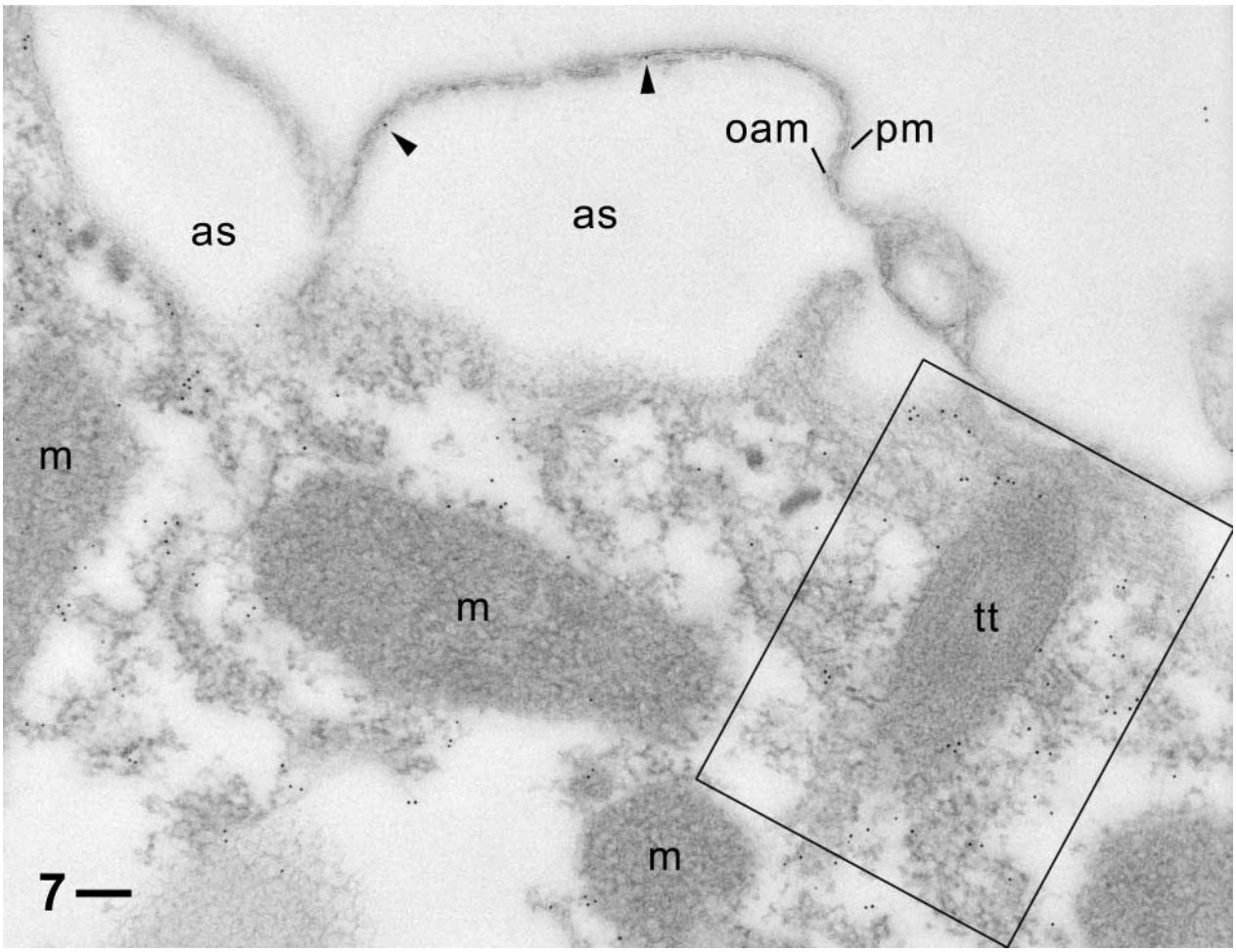

Figure 7 Similar situation as in Figures 5 and 6, but with more clearly visible label (rectangle) particularly surrounding a longitudinally cut trichocyst tip (tt) and occasional label (arrowheads) in the very narrow subplasmalemmal space between the plasma membrane (pm) and the outer alveolar sacs membrane (oam). Note absence of label from the off-cell region, alveolar sacs (as), and mitochondria (m). Bar = 0.1 μm.

uble antigen relocation and even loss during permeabilization. This would not easily be possible with the postembedding immuno-EM labeling procedure used now. Another hint to real cortical F-actin localization in *Paramecium* came from the in vivo labeling by injection of fluorescent phalloidin (Kersken et al. 1986a,b), resulting first in cortical labeling and, over longer time periods, in disappearance from the cortex and re-assembly as thick trans-cellular filament bundles of a type not previously seen. Conversely, aberrant phalloidin binding by F-actin formed by some isoforms may preclude labeling (Hirono et al. 1989), while such forms may bind actin-specific ABs.

Additional Functional Aspects Derived from This Study

Cortical F-actin is generally required for cyclosis—an actomyosin-based process (Shimmen and Yokota 2004). This is a permanent ongoing process also in *Paramecium* (Sikora et al. 1979), where it serves the delivery of trichocysts to the cell cortex (Aufderheide 1977) and the cycling of phago-lysosomal elements through the cell body (Fok and Allen 1988,1990; Allen and Fok 2000). Myosins occur in *Paramecium* (Cohen et al. 1987), just as in other protists (Gavin 2001).

Our present EM analysis verifies that in the *Paramecium* cell cortex, actin is enriched at ciliary basal bodies, as discussed above on the LM level. From there it emanates to the infraciliary lattice and around trichocyst docking sites. The association of actin with ciliary basal bodies has led to the description of the "basal body cage," particularly in *Tetrahymena* (Hoey and Gavin 1992), where association with myosin has been demonstrated (Garcés et al. 1995). The loose arrangement of gold label within and around basal bodies, as we see it here, suggests that during permeabilization for LM analysis, F-actin emanating from basal bodies may collapse to a compact arrangement. In

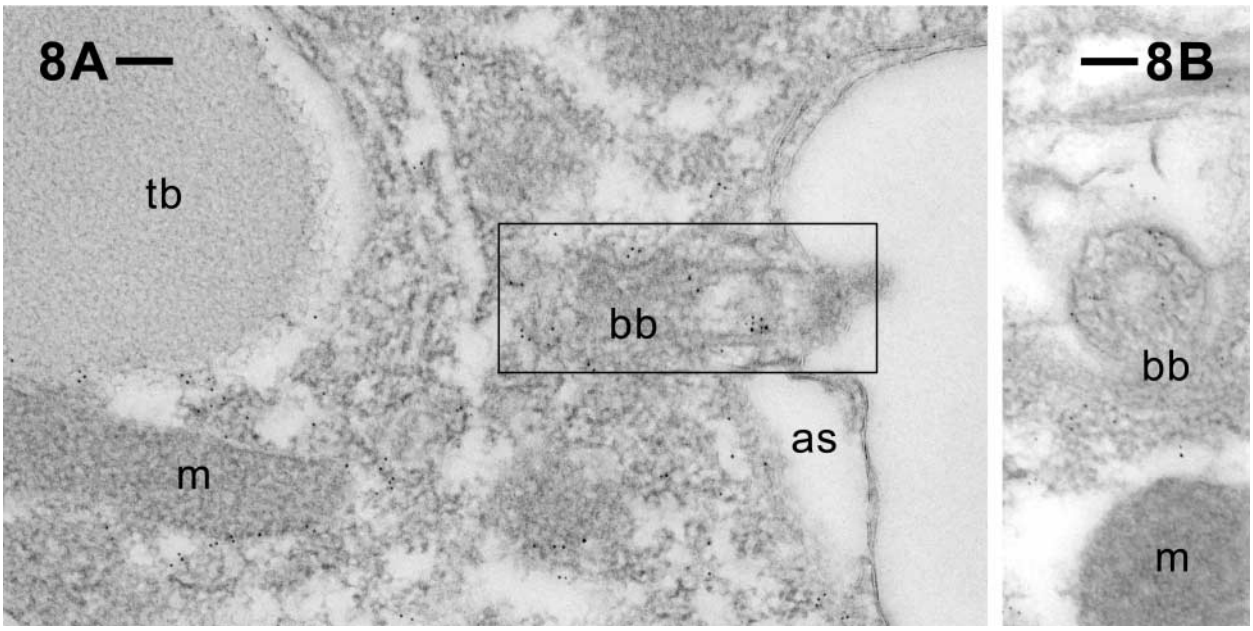

Figure 8 Postembedding immunogold labeling of ciliary basal bodies (bb) located on the outer cell surface, in longitudinal (**A**) and in cross-section (**B**), with additional label on diffuse materials surrounding the basal body (framed in **A**). Note again absence of label on irrelevant structures, such as alveolar sacs (as), mitochondria (m) and a trichocyst body (tb). Bars = 0.1 μm.

sum, a more loosely arranged cortical F-actin in conjunction with myosin may underlie cytoplasmic streaming and possibly trichocyst docking. Concomitantly, inhibition of trichocyst docking by cytochalasin B (Beisson and Rossignol 1975) would be compatible with both actin-based transport by cyclosis and enrichment of actin around trichocyst tips (this study).

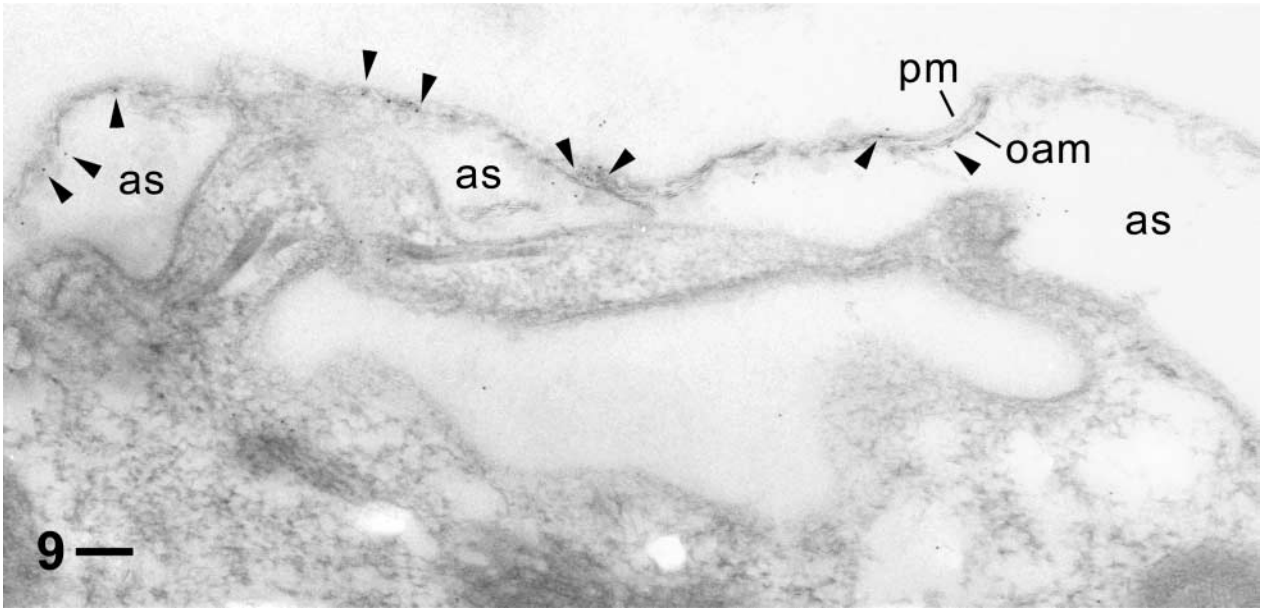

Figure 9 Combination of pre- and postembedding immunolabeling shows label in the narrow subplasmalemmal space (at/between arrowheads) between the plasma membrane (pm) and the outer alveolar sacs (as) membrane (oam), with little background on irrelevant structures outside the cytosolic compartment. Note deformation of the cell surface membrane complex (pm/oam), with some label attached particularly in regions with a "grazing" section plane, due to the permeabilization applied. This cell has been digitonized during aldehyde fixation for impregnation with primary AB and IgG-Au_5 and embedded for incubation with the same ABs in sequence. Bar = 0.1 μm.

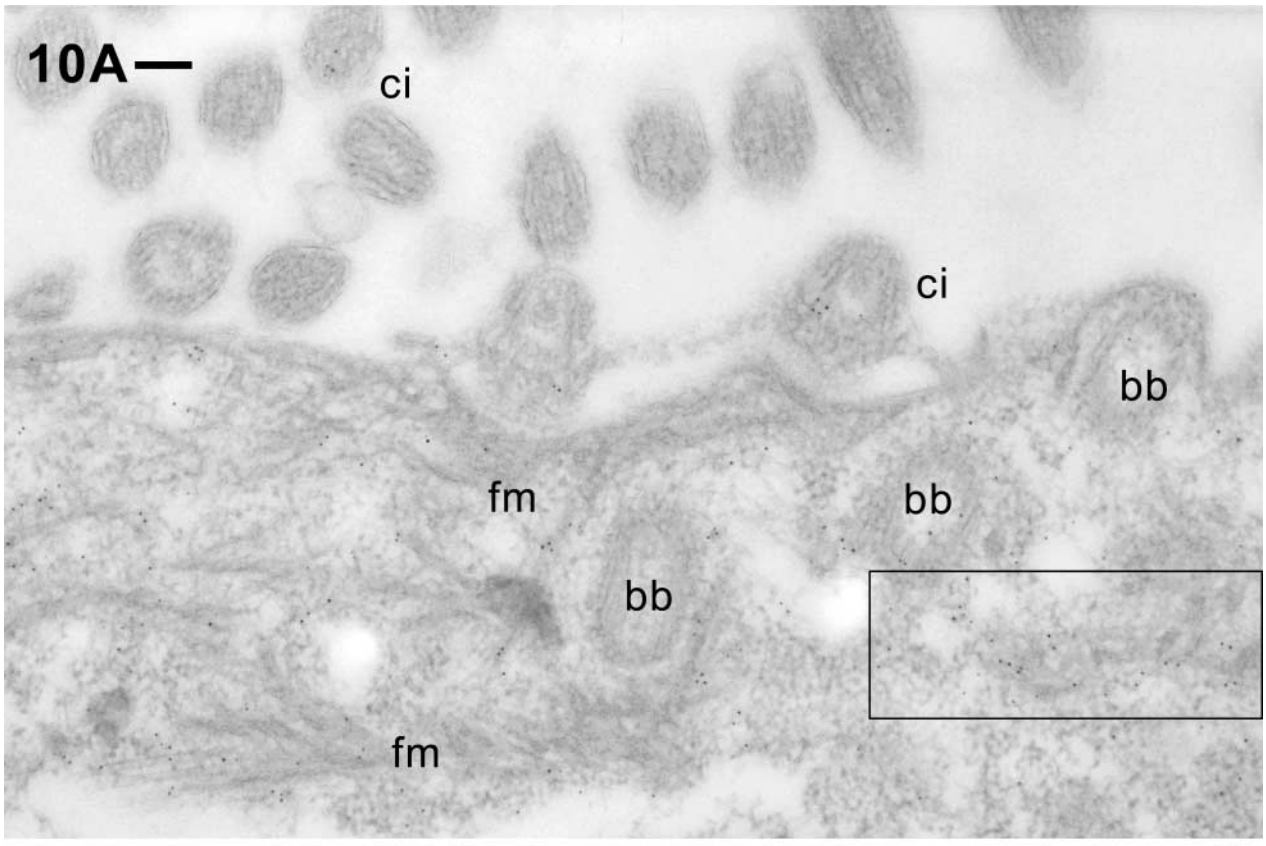
10A
ci
ci
bb
fm
bb
bb
fm

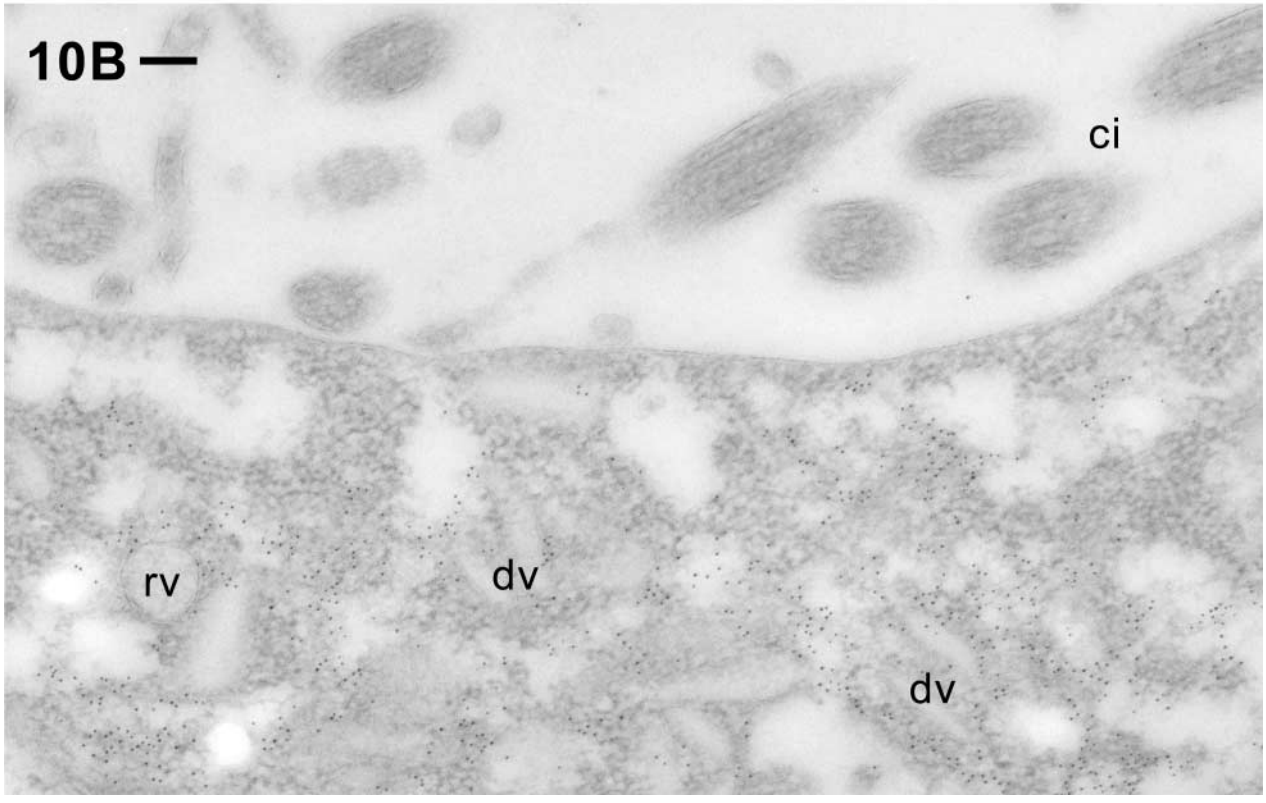
10B
ci
rv
dv
dv

Assembly of F-actin around nascent phagosomes is well established, not only in mammalian cells but also in *Paramecium* cells (Allen and Fok 1983; Fok and Allen 1988). In detail, fusion of acidosomes with the nascent food vacuole depends on F-actin (Fok et al. 1987), as does maturation along the phago-lysosomal pathway, where multiple fusion/fission processes occur (Allen and Fok 1985; Allen et al. 1995). Interestingly, in our study, gold labeling immediately below the cytopharyngeal plasma membrane is less intense than between the closely packed globular and discoidal vesicles slightly below. This can be seen in line with the following reports. In *Dictyostelium*, F-actin prevents clustering of endosomal vacuoles (Drengk et al. 2003). Alternatively, in yeast, actin is required for Ca^{2+}-mediated vacuole interaction leading to fusion (Merz and Wickner 2004). The final step of this cycle in *Paramecium*, exocytotic release of spent phagolysosomes, can also be inhibited by cytochalasin B (Allen and Fok 1985). In agreement with this previous work, the site of phagosome formation, vacuoles of different size, and the cytoproct are clearly labeled with anti-actin ABs in our CLSM and EM pictures. Therefore, the fine filaments described at the cytoproct by Cohen et al. (1984) are, at least to some extent, F-actin. However, centrin also occurs at the cytoproct, according to the CLSM pictures presented in Figure 3.

At the EM level, we see that the cytosolic compartment around large and small vacuoles is frequently heavily labeled (even when filaments are difficult to discern due to faint contrast resulting from preparation for immuno-EM analysis). This holds, e.g., for domains with clearly visible microtubule bundles deep inside the cell and for regions with discoidal vesicles approaching the cytopharynx. The latter are delivered along microtubule rails, using dynein as a motor (Schroeder et al. 1990). Therefore, actin at these sites may serve not as a motor, but rather as a kind of scaffold. In sum, apart from association with non-actin filaments (see below), we see that actin is also associated with the second cytoskeletal element, the microtubules. This agrees with functional data obtained by combined drug application (Fok et al. 1985).

Label also occurs around the oral cavity outside the site of phagosome formation in the cytopharynx. Such filaments are known not to represent actin, either in *Paramecium* (Clérot et al. 2001), or in other ciliates (Viguès et al. 1999). In these regions, F-actin may again serve structuring of these firmly established subcellular domains and/or vesicle trafficking. Interestingly, co-assembly of polymerizing actin with other filament components from *Tetrahymena* can be produced in vitro (Mitchell and Zimmerman 1985).

Vesicles deeper inside the cytoplasm, often close to a large phagosome, are also surrounded by gold label. All this reflects that actin is present throughout the cell in LM analyses, frequently as strands. Actin may thus participate directly or indirectly in vesicle trafficking, including cyclosis.

Not only ciliary basal bodies, but also the ciliary shaft, are labeled by anti-actin ABs. Labeling of cilia has been reported previously based on peroxidase-based preembedding immunostaining in *Paramecium* (Tiggemann and Plattner 1981) and in quail oviducts (Sandoz et al. 1982). Because this method is subject to redistribution artifacts (Plattner and Zingsheim 1983), we considered a re-analysis by Western blots and by the postembedding EM methodology to be necessary. It is known only from flagella of the green alga, *Chlamydomonas* (Mitchell 2000; Hayashi et al. 2001; Hirono et al. 2003), that actin is mandatory for normal beat activity. This may apply also to cilia of *Tetrahymena*, whose 14S axonemal dynein binds actin (Muto et al. 1994). More details on the role of actin in cilia remain to be elucidated.

Another poorly understood aspect concerns coupling of cortical calcium stores to the cell membrane. With mammalian cells, one of the molecules considered to establish such connections, particularly for store-operated Ca^{2+}-influx, is actin (Patterson et al. 1999; Rosado and Sage 2000; Kunzelmann-Marche et al. 2001; Wang et al. 2002). Interestingly, we find gold label that may be associated with the narrow subplasmalemmal space not only using a variation of the general labeling procedure that faciliates access of ABs (Figure 9), but also, though to a lesser extent, using postembedding labeling (Figures 5 and 7). This becomes evident particularly after statistical evaluation (Table 1). Although cytochalasin B application did not change concomittant Ca^{2+} signals (Mohamed et al. 2003), we keep this question open because the different actin isoforms found in *Paramecium* (Kissmehl et al., in preparation) may have different drug sensitivities.

Figure 10 Label around the oral cavity, in a region enriched in ciliary basal bodies (bb) in (**A**) or in vesicles (**B**). These represent, at least in part, discoidal vesicles (dv) known to recycle membranes for nascent phagosome formation, which may be assisted by round vesicles (rv) as discussed in the text. A particularly densely labeled domain in (**A**) is framed. Some label is located between unlabeled fibrous material (fm, not actin-type). Also note some label on basal bodies (bb) and within some cilia (ci). In (**B**), the label is scattered between the discoidal vesicles (dv). In (**A**) and (**B**), a $\geq$1-μm-thick layer below the oral cavity plasma membrane is heavily labeled, starting at a distance from the plasma membrane. Bars = 0.1 μm.

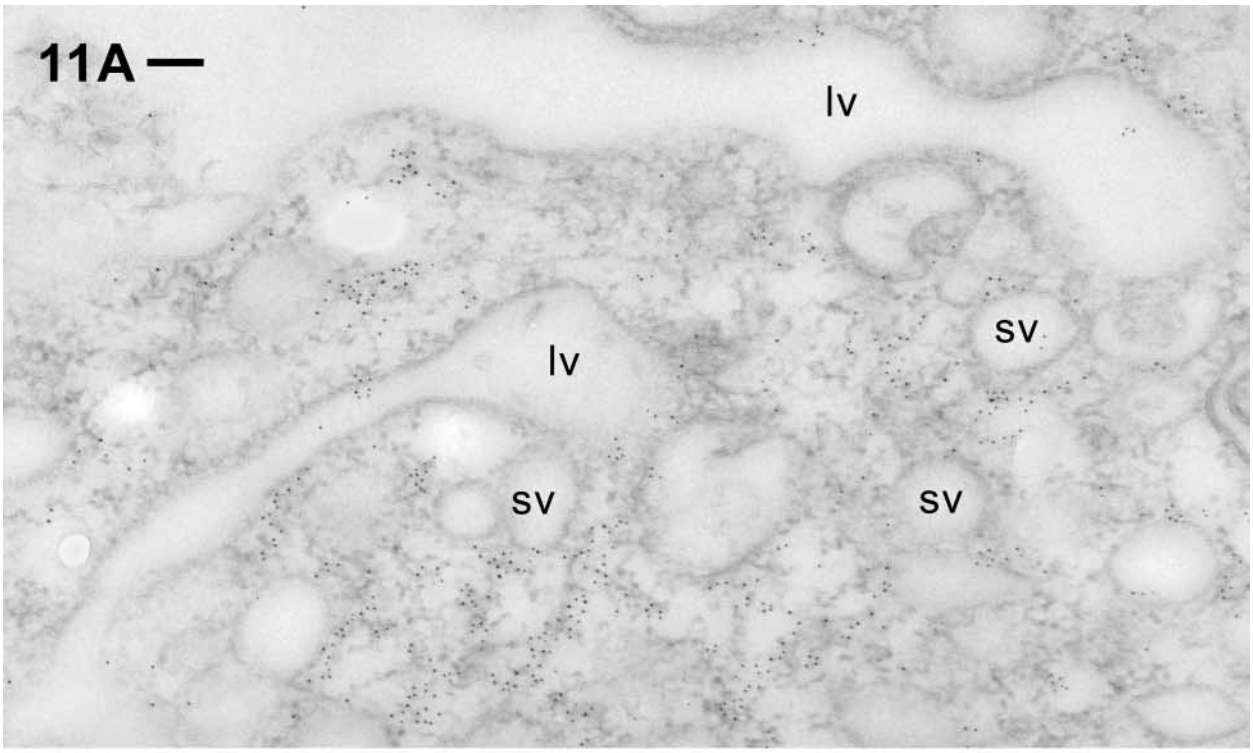
11A —
lv
lv
sv
sv
sv

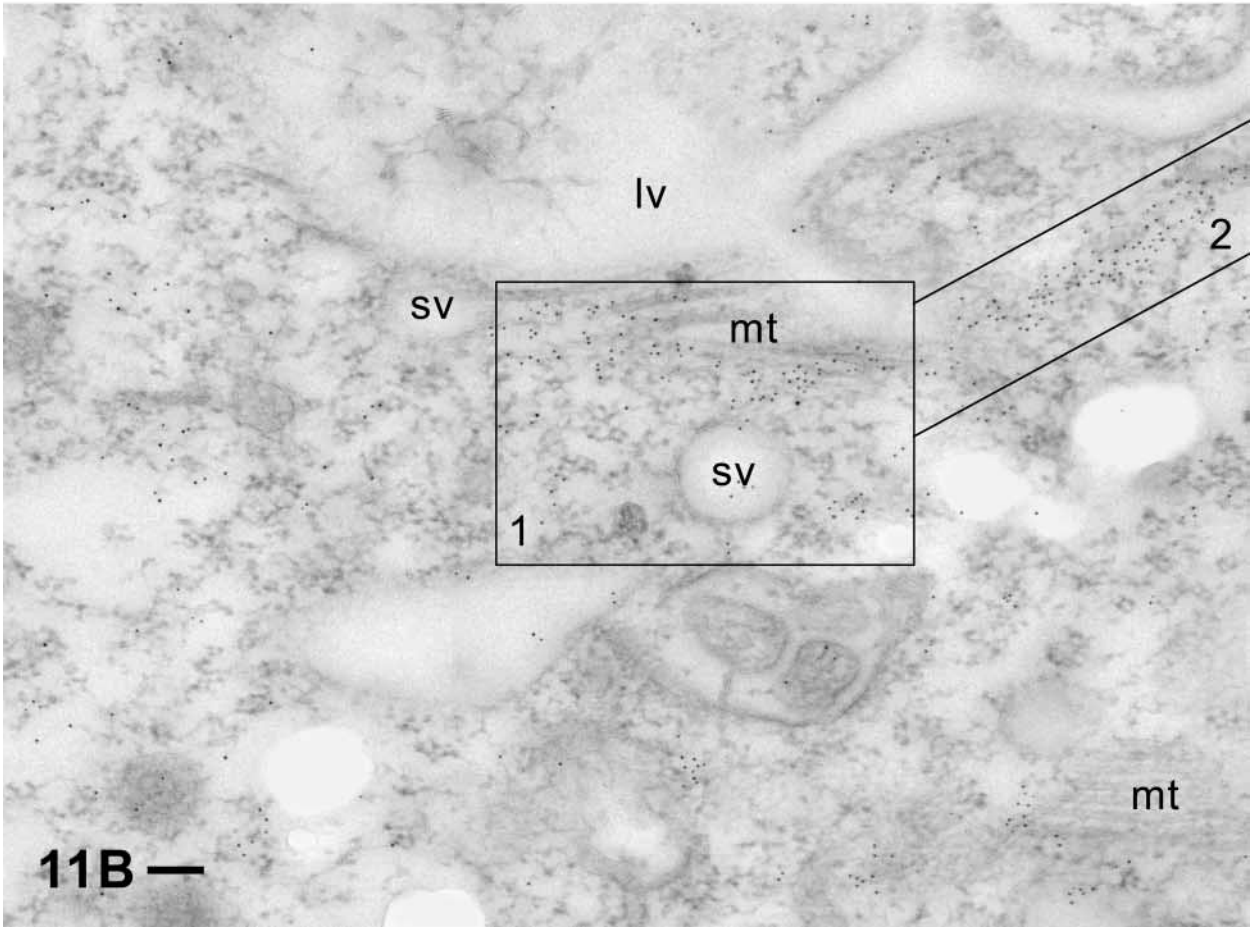
lv
2
sv
mt
sv
1
mt
11B —

Table 1 Labeling density (gold grains/μm^2) achieved with anti-actin AB/gold conjugate over different structural components, background [2.15 ± 0.85 (SEM), $n = 6$, determined off cell, or in the lumen of food vacuoles] subtracted

Structure analyzed	Gold grains/mm2	6SEM	*n*
Cilia	89.5	±25.5	21
Basal bodies	91.0	±24.9	12
Plasma membrane/outer alveolar membrane complex	25.9	±4.1	14
Cell surface "ridges"	141.5	±56.8	6
Alveolar sacs contents	0.3	±0.3	21
Cortical cytoplasm	37.8	±4.9	5
Infraciliary lattice	95.6	±6.2	3
Surroundings of trichocyst tips	111.9	±27.0	7
Trichocyst contents	1.4	±0.8	8
Mitochondria	2.2	±1.0	11
Small vesicles associated with oral cavity and around food vacuoles	7.0	±7.0	63
Cytoplasmic regions around oral cavity and around food vacuoles	301.0	±7.6	2

SEM = standard error of the mean; n = number of structural components analyzed.

Our present immunogold EM analysis largely depends on the preparation schedule used, whereas we obtained no such clear-cut labeling pattern with other approaches (data not shown). The current approach implied rapid injection (spraying) of cells in 0C aldehyde fixative, containing high formaldehyde and very low glutaraldehyde concentrations, followed by low temperature embedding and UV polymerization at −35C. This can considerably restrict diffusion of macromolecules and, even more, of filamentous aggregates. Therefore, we consider the current approach, elaborated on a (semi-)quantitative basis, more reliable than some previous attempts to localize actin in such cells.

Acknowledgments

We gratefully acknowledge the kind help of Dr R. Gräf (University of Munich) for a gift of anti-centrin ABs, as well as the help of our group members, of Dr Joachim Hentschel with the quenched-flow preparations, and the skillful technical assistance of Ms Lauretta Schade in the EM documentation. We thank Dr Claudia Stuermer for access to the CLSM and Ms Sylvia Hannbeck von Hanwehr for technical help in the CLSM analysis, as well as Ms Doris Bliestle for electronic image processing. Supported by grants from the Deutsche Forschungsgemeinschaft to HP.

Literature Cited

Allen RD (1971) Fine structure of membranous and microfibrillar systems in the cortex or *Paramecium caudatum*. J Cell Biol 49: 1–20

Allen RD (1988) Cytology. In Görtz HD, ed. *Paramecium*. Heidelberg, New York, London, Paris, Tokyo, Springer Verlag, 4–40

Allen RD, Aihara MS, Fok AK (1998) The striated bands of *Paramecium* are immunologically distinct from the centrin-specific infraciliary lattice and cytostomal cord. J Eukaryot Microbiol 45: 202–209

Allen RD, Bala NP, Ali RF, Nishida DM, Aihara MS, Ishida M, Fok AK (1995) Rapid bulk replacement of acceptor membrane by donor membrane during phagosome to phagoacidosome transformation in *Paramecium*. J Cell Sci 108:1263–1274

Allen RD, Fok AK (1983) Nonlysosomal vesicles (acidosomes) are involved in phagosome acidification in *Paramecium*. J Cell Biol 97:566–570

Allen RD, Fok AK (1985) Modulation of the digestive lysosomal system in *Paramecium caudatum*. III. Morphological effects of cytochalasin B. Eur J Cell Biol 37:35–43

Allen RD, Fok AK (2000) Membrane trafficking and processing in *Paramecium*. Int Rev Cytol 198:277–318

Aufderheide KJ (1977) Saltatory motility of uninserted trichocysts and mitochondria in *Paramecium tetraurelia*. Science 198:299–300

Beisson J, Clérot JC, Fleury-Aubusson A, Garreau De Loubresse N, Ruiz F, Klotz C (2001) Basal body-associated nucleation center for the centrin-based cortical cytoskeletal network in *Paramecium*. Protist 152:339–354

Beisson J, Rossignol M (1975) Movements and positioning of organelles in *Paramecium aurelia*. In Puiseux-Dao S, ed. Nucleocytoplasmic Relationships during Cell Morphogenesis in Some Unicellular Organisms. Amsterdam, New York, London, Elsevier Publishing Company, 291–294

Bubb MR, Spector I, Beyer BB, Fosen KM (2000) Effects of jasplakinolide on the kinetics of actin polymerization. An explanation for certain in vivo observations. J Biol Chem 275:5163–5170

Clérot JC, Iftode F, Budin K, Jeanmaire-Wolf R, Coffe G, Fleury-Aubusson A (2001) Fine oral filaments in *Paramecium*: a biochemical and immunological analysis. J Eukaryot Microbiol 48: 234–245

Cohen J, Beisson J (1988) The cytoskeleton. In Görtz HD, ed. *Paramecium*. Heidelberg, New York, London, Paris, Tokyo, Springer Verlag, 363–392

Cohen J, Garreau De Loubresse N, Beisson J (1984) Actin microfilaments in *Paramecium*: localization and role in intracellular movements. Cell Motil 4:443–468

Figure 11 Label of the cytosolic compartment around small vacuoles (sv), probably acidosomes, approaching a large one (lv), probably a nascent food vacuole (see text). Particularly labeled domains are highlighted (boxes 1, 2). Some of this label is associated with microtubule bundles (mt), e.g., in (**B**), but not in (**A**). In (**B**) a "trail" marked by box 2 is especially strongly labeled, although no distinct filament system can be recognized because of the preparation required. Only occasional gold grains are seen in non-cytosolic compartments, e.g., background in vacuole in (**A**). Bars = 0.1 μm.

Cohen J, Garreau De Loubresse N, Klotz C, Ruiz F, Bordes N, Sandoz D, Bornens M, et al. (1987) Organization and dynamics of a cortical fibrous network of *Paramecium*: the outer lattice. Cell Motil Cytoskel 7:315–324

Cupples CG, Pearlman RE (1986) Isolation and characterization of the actin gene from *Tetrahymena thermophila*. Proc Natl Acad Sci USA 83:5160–5164

Daunderer C, Schliwa M, Gräf R (2001) *Dictyostelium* centrin-related protein (DdCrp), the most divergent member of the centrin family, possesses only two EF hands and dissociates from the centrosome during mitosis. Eur J Cell Biol 80:621–630

Delbac F, Sänger A, Neuhaus EM, Stratmann R, Ajioka JW, Toursel C, Herm-Götz A, et al. (2001) *Toxoplasma gondii* myosins B/C: one gene, two tails, two localizations, and a role in parasite division. J Cell Biol 155:613–623

Dessen P, Zagulski M, Gromadka R, Plattner H, Kissmehl R, Meyer E, Betermier M, et al. (2001) *Paramecium* genome survey: a pilot project. Trends Genet 17:306–308

Díaz-Ramos C, Villalobo E, Pérez-Romero P, Torres A (1998) *Paramecium tetraurelia* encodes unconventional actin containing short introns. J Eukaryot Microbiol 45:507–511.

Drengk A, Fritsch J, Schmauch C, Rühling H, Maniak M (2003) A coat of filamentous actin prevents clustering of late-endosomal vacuoles in vivo. Curr Biol 13:1814–1819

Engqvist-Goldstein AEY, Drubin DG (2003) Actin assembly and endocytosis: from yeast to mammals. Annu Rev Cell Dev Biol 19:287–332

Fahrni JF (1992) Actin in the ciliated protozoan *Climacostomum virens*: purification by DNAse I affinity chromatography, electrophoretic characterization, and immunological analysis. Cell Motil Cytoskel 22:62–71

Fok AK, Allen RD (1988) The lysosome system. In Görtz HD, ed. *Paramecium*. Berlin, Heidelberg, New York, London, Paris, Tokyo, Springer Verlag, 301–324

Fok AK, Allen RD (1990) The phagosome-lysosome membrane system and its regulation in *Paramecium*. Int Rev Cytol 123:61–94

Fok AK, Leung SSK, Chun DP, Allen RD (1985) Modulation of the digestive lysosomal system in *Paramecium caudatum*. II. Physiological effects of cytochalasin B, colchicine and trifluoperazine. Eur J Cell Biol 37:27–34.

Fok AK, Ueno MS, Azada EA, Allen RD (1987) Phagosomal acidification in *Paramecium*: effects on lysosomal fusion. Eur J Cell Biol 43:412–420.

Garcés JA, Hoey JG, Gavin RH (1995) Putative myosin heavy and light chains in *Tetrahymena*: co-localization to the basal body-cage complex and association of the heavy chain with skeletal muscle actin filaments in vitro. J Cell Sci 108:869–881.

Gasman S, Chasserot-Golaz S, Malacombe M, Way M, Bader MF (2004) Regulated exocytosis in neuroendocrine cells: a role for subplasmalemmal Cdc42/N-WASP-induced actin filaments. Mol Biol Cell 15:520–531.

Gavin RH (2001) Myosins in protists. Int Rev Cytol 206:97–134.

Glas-Albrecht R, Plattner H (1990) High yield isolation procedure for intact secretory organelles (trichocysts) from *Paramecium tetraurelia* strains. Eur J Cell Biol 53:164–172.

Guilherme A, Soriano NA, Bose S, Holik J, Bose A, Pomerleau DP, Furcinitti P, et al. (2004) EDH2 and the novel EH domain binding protein EHBP1 couple endocytosis to the actin cytoskeleton. J Biol Chem 279:10593–10605

Hauser M, Hausmann K, Jockusch BM (1980) Demonstration of tubulin, actin and α-actinin by immunofluorescence in the microtubule-microfilament complex of the cytopharyngeal basket of the ciliate *Pseudomicrothorax dubius*. Exp Cell Res 125:265–274.

Hayashi M, Hirono M, Kamiya R (2001) Recovery of flagellar dynein function in a *Chlamydomonas* actin/dynein-deficient mutant upon introduction of muscle actin by electroporation. Cell Motil Cytoskel 49:146–153

Hirono M, Endoh H, Okada N, Numata O, Watanabe Y (1987a) *Tetrahymena* actin. Cloning and sequencing of the *Tetrahymena* actin gene and identification of its gene product. J Mol Biol 194: 181–192

Hirono M, Kumagai Y, Numata O, Watanabe Y (1989) Purification of *Tetrahymena* actin reveals some unusual properties. Proc Natl Acad Sci USA 86:75–79

Hirono M, Nakamura M, Tsunemoto M, Yasuda T, Ohba H, Numata O, Watanabe Y (1987b) *Tetrahymena* actin: localization and possible biological roles of actin in *Tetrahymena* cells. J Biochem 102:537–545

Hirono M, Uryu S, Ohara A, Kato-Minoura T, Kamiya R (2003) Expression of conventional and unconventional actins in *Chlamydomonas reinhardtii* upon deflagellation and sexual adhesion. Eukaryot Cell 2:486–493

Hoey JG, Gavin RH (1992) Localization of actin in the *Tetrahymena* basal body-cage complex. J Cell Sci 103:629–641

Kaneshiro ES, Beischel LS, Merkel SJ, Rhoads DE (1979) The fatty acid composition of *Paramecium aurelia* cells and cilia: changes with culture age. J Protozool 26:147–158.

Kersken H, Momayezi M, Braun C, Plattner H (1986a) Filamentous actin in *Paramecium* cells: functional and ultrastructural changes correlated with phalloidin affinity labeling in vivo. J Histochem Cytochem 34:455–465

Kersken H, Vilmart-Seuwen J, Momayezi M, Plattner H (1986b) Filamentous actin in *Paramecium* cells: mapping by phalloidin affinity labeling in vivo and in vitro. J Histochem Cytochem 34: 443–454

Keryer G, Adoutte A, Ng SF, Cohen J, Garreau De Loubresse N, Rossignol M, Stelly N, et al. (1990a) Purification of the surface membrane-cytoskeleton complex (cortex) of *Paramecium* and identification of several of its protein constituents. Eur J Protistol 25:209–225

Keryer G, Iftode F, Bornens M (1990b) Identification of proteins associated with microtubule-organizing centres and filaments in the oral apparatus of the ciliate *Paramecium tetraurelia*. J Cell Sci 97:553–563

Kissmehl R, Treptau T, Hofer HW, Plattner H (1996) Protein phosphatase and kinase activities possibly involved in exocytosis regulation in *Paramecium tetraurelia*. Biochem J 317:65–76

Kjeken R, Egeberg M, Habermann A, Kuehnel M, Peyron P, Floetenmeyer M, Walther P, et al. (2004) Fusion between phagosomes, early and late endosomes: a role for actin in fusion between late, but not early endocytic organelles. Mol Biol Cell 15: 345–358

Klotz C, Garreau de Loubresse N, Ruiz F, Beisson J (1997) Genetic evidence for a role of centrin-associated proteins in the organization and dynamics of the infraciliary lattice in *Paramecium*. Cell Motil Cytoskel 38:172–186

Knoll G, Braun C, Plattner H (1991) Quenched flow analysis of exocytosis in *Paramecium* cells: time course, changes in membrane structure, and calcium requirements revealed after rapid mixing and rapid freezing of intact cells. J Cell Biol 111:1295–1304

Kunzelmann-Marche C, Freyssinet JM, Martínez MC (2001) Regulation of phosphatidylserine transbilayer redistribution by store-operated Ca^{2+} entry. Role of actin cytoskeleton. J Biol Chem 276:5134–5139

Kyhse-Andersen J (1989) Multi-chamber apparatus for preparative isoelectric focusing. Electrophoresis 10:6–10

Laemmli UK (1970) Cleavage of structural proteins during the assembly of the head of bacteriophage T4. Nature 227:680–685

Lumpert CJ, Kersken H, Plattner H (1990) Cell surface complexes ('cortices') isolated from *Paramecium tetraurelia* cells as a model system for analysing exocytosis in vitro in conjunction with microinjection studies. Biochem J 269:639–645

Manneville JB, Etienne-Manneville S, Skehel P, Carter T, Ogden D, Ferenczi M (2003) Interaction of the actin cytoskeleton with microtubules regulates secretory organelle movement near the plasma membrane in human endothelial cells. J Cell Sci 116: 3927–3938.

Merz AJ, Wickner WT (2004) Trans-SNARE interactions elicit Ca^{2+} efflux from the yeast vacuole lumen. J Cell Biol. 164:195–206

Méténier G (1984) Actin in *Tetrahymena paravorax*: ultrastructural localization of HMM-binding filaments in glycerinated cells. J Protozool 31:205–215

Mitchell DR (2000) *Chlamydomonas* flagella. J Phycol 36:261–273
Mitchell EJ, Zimmerman AM (1985) Biochemical evidence for the presence of an actin protein in *Tetrahymena pyriformis*. J Cell Sci 73:279–297
Mohamed I, Husser M, Sehring I, Hentschel J, Hentschel C, Plattner H (2003) Refilling of cortical calcium stores in *Paramecium* cells: in situ analysis in correlation with store-operated calcium influx. Cell Calcium 34:87–96
Morales M, Colicos MA, Goda Y (2000) Actin-dependent regulation of neurotransmitter release at central synapses. Neuron 27: 539–550
Muto E, Edamatsu M, Hirono M, Kamiya R (1994) Immunological detection of actin in the 14S ciliary dynein of *Tetrahymena*. FEBS Lett 343:173–176
Nelson DL (1995) Preparation of cilia and subciliary fractions from *Paramecium*. Methods Cell Biol 47:17–24
Pape R, Plattner H (1990) Secretory organelle docking at the cell membrane of *Paramecium* cells: dedocking and synchronized redocking of trichocysts. Exp Cell Res 191:263–272
Patterson RL, Van Rossum DB, Gill DL (1999) Store-operated Ca^{2+} entry: evidence for a secretion-like coupling model. Cell 98:487–499
Pendleton A, Koffer A (2001) Effects of latrunculin reveal requirements for the actin cytoskeleton during secretion from mast cells. Cell Motil Cytoskel 48:37–51
Pérez-Romero P, Villalobo E, Díaz-Ramos C, Calvo P, Torres A (1999) Actin of *Histriculus cavicola*: characteristics of the highly divergent hypotrich ciliate actins. J Eukaryot Microbiol 46:469–472
Plattner H, Klauke N (2001) Calcium in ciliated protozoa: sources, regulation, and calcium-regulated cell functions. Int Rev Cytol 201:115–208
Plattner H, Zingsheim HP (1983) Electron microscopic methods in cellular and molecular biology. Subcell Biochem 9:1–236
Pollard TD, Blanchoin L, Mullins RD (2000) Molecular mechanisms controlling actin filament dynamics in nonmuscle cells. Annu Rev Biophys Biomol Struct 29:545–576
Poupel O, Boleti H, Axisa S, Couture-Tosi E, Tardieux I (2000) Toxofilin, a novel actin-binding protein from *Toxoplasma gondii*, sequesters actin monomers and caps actin filaments. Mol Biol Cell 11:355–368
Rosado JA, Sage SO (2000) The actin cytoskeleton in store-mediated calcium entry. J Physiol 526:221–229
Sanders MA, Salisbury JL (1994) Centrin plays an essential role in microtubule severing during flagellar excision in *Chlamydomonas reinhardtii*. J Cell Biol 124:795–805
Sandoz D, Gounon P, Karsenti E, Sauron ME (1982) Immunocytochemical localization of tubulin, actin, and myosin in axonemes of ciliated cells from quail oviduct. Proc Natl Acad Sci USA 79:3198–3202
Schroeder CC, Fok AK, Allen RD (1990) Vesicle transport along microtubular ribbons and isolation of cytoplasmic dynein from *Paramecium*. J Cell Biol 111:2553–2562
Shimmen T, Yokota E (2004) Cytoplasmic streaming in plants. Curr Opinion Cell Biol 16:68–72
Sibley LD (2004) Intracellular parasite invasion strategies. Science 304:248–253
Sikora J, Wasik A, Baranowski Z (1979) The estimation of velocity distribution profile of *Paramecium* cytoplasmic streaming. Eur J Cell Biol 19:184–188
Sonneborn TM (1970) Methods in *Paramecium* research. Methods Cell Physiol 4:242–335
Sperling LP, Dessen P, Zagulski M, Pearlman RE, Migdalski A, Gromadka R, Froissard M, et al. (2002) Random sequencing of *Paramecium* somatic DNA. Eukaryot. Cell 1:341–352
Starr DA, Han M (2003) ANChors away: an actin based mechanism of nuclear positioning. J Cell Sci 116:211–216
Stoorvogel W, Kerstens S, Fritzsche I, Den Hartigh JC, Oud R, Van Der Heyden MAG, Voortman J, et al. (2004) Sorting of ligand-activated epidermal growth factor receptor to lysosomes requires its actin-binding domain. J Biol Chem 279:11562–11569
Tiggemann R, Plattner H (1981) Localization of actin in the cortex of *Paramecium tetraurelia* cells by immuno- and affinity-fluorescence microscopy. Eur J Cell Bio 24:184–190
Valentijn K, Valentijn JA, Jamieson JD (1999) Role of actin in regulated exocytosis and compensatory membrane retrieval: insights from an old acquaintance. Biochem Biophys Res Commun 266: 652–661
Viguès B, Blanchard MP, Bouchard P (1999) Centrin-like filaments in the cytopharyngeal apparatus of the ciliates *Nassula* and *Furgasonia*: evidence for a relationship with microtubular structures. Cell Motil Cytoskel 43:72–81
Wagner CR, Mahowald AP, Miller KG (2002) One of the two cytoplasmic actin isoforms in *Drosophila* is essential. Proc Natl Acad Sci USA 99:8037–8042
Wang YJ, Gregory RB, Barritt GJ (2002) Maintenance of the filamentous actin cytoskeleton is necessary for the activation of store-operated Ca^{2+} channels, but not other types of plasmamembane Ca^{2+} channels, in rat hepatocytes. Biochem J 363:117–126
Wetzel DM, Hakansson S, Hu K, Roos D, Sibley LD (2003) Actin filament polymerization regulates gliding motility by apicomplexan parasites. Mol Biol Cell 14:396–406
Wieland T, Faulstich H (1978) Amatoxins, phallotoxins, phallolysin, and antamanide: the biologically active components of poisonous *Amanita* mushrooms. Crit Rev Biochem 5:185–260
Zackroff RV, Hufnagel LA (1998) Relative potencies of different cytochalasins for the inhibition of phagocytosis in ciliates. J Eukaryot Microbiol 45:397–403
Zackroff RV, Hufnagel LA (2002) Induction of anti-actin drug resistance in *Tetrahymena*. J Eukaryot Microbiol 49:475–477
Zimmerman AM, Zimmerman S, Thomas J, Ginzburg I (1983) Control of tubulin and actin gene expression in *Tetrahymena pyriformis* during the cell cycle. FEBS Lett 164:318–322